Estuarine, Coastal and Shelf Science 116 (2013) 87–98

Contents lists available at SciVerse ScienceDirect

Estuarine, Coastal and Shelf Science

journal homepage: www.elsevier.com/locate/ecss

Management modeling of suspended solids in the Chesapeake Bay, USA

Carl F. Cerco [a,*], Sung-Chan Kim [b], Mark R. Noel [a]

[a] Environmental Laboratory, US Army Engineer Research and Development Center, 3909 Halls Ferry Road, Vicksburg, MS 39180, USA
[b] Coastal and Hydraulics Laboratory, US Army Engineer Research and Development Center, 3909 Halls Ferry Road, Vicksburg, MS 39180, USA

ARTICLE INFO

Article history:
Received 30 November 2011
Accepted 13 July 2012
Available online 24 July 2012

Keywords:
estuaries
eutrophication
suspended particulate matter
light attenuation
models

ABSTRACT

The Chesapeake Bay, USA, suffers from multiple water quality impairments including poor water clarity. A management strategy aimed at improving water clarity through reduction of nutrient and solids loads to the bay is under development. The strategy is informed through the use of the Chesapeake Bay Environmental Modeling Package. We describe herein aspects of the model devoted to suspended solids, a major contributor to poor water clarity. Our approach incorporates a dynamic model of inorganic solids into an eutrophication model, in order to account for interactions between physical and biotic factors which influence suspended solids transport and fate. Solids budgets based on the model indicate that internal production of organic solids is the largest source of suspended solids to the mainstem bay. Scenario analysis indicates that control of solids loads reduces solids concentration in the vicinity of the loading sources. Control of nutrient loads provides more widespread but lesser reductions in suspended solids.

Published by Elsevier Ltd.

1. Introduction

Chesapeake Bay is the largest estuary in the United States. The physical characteristics and the environmental problems prevalent in the bay have been described extensively (Hagy et al., 2004; Kemp et al., 2005) and are repeated only briefly here. The mainstem of the bay (Fig. 1) is a drowned river valley which extends roughly 300 km from the Atlantic Ocean to the Susquehanna River. The bay channel achieves depths of 30 m but adjoins extensive shoal areas so that the average depth is ≈6 m. The Susquehanna River provides the majority (≈60%) of the freshwater to the bay. The remainder is primarily from five major western tributaries. The bay is described as partially-mixed and demonstrates classic estuarine circulation in which residual flow is predominantly downstream at the surface and upstream near the bottom. The actions of wind and other climatic events can interrupt this classic pattern, however. Salinity ranges from nearly oceanic, at the mouth, to freshwater in the vicinity of the Susquehanna. The mean tide range is 0.78 m at the mouth and decreases to less than 0.4 m in the upper bay.

Chesapeake Bay exhibits multiple signs of cultural eutrophication, which has accelerated since the 1950s. Primary among these are resource depletion (Newell, 1988), bottom-water anoxia (Hagy et al., 2004), and disappearance of submerged aquatic vegetation (SAV, Orth and Moore, 1983). The modern era of water quality management in the bay commenced in the early 1980s with the formation of the US EPA Chesapeake Bay Program (CBP). Formation of the CBP coincided with widespread publicity about deteriorating conditions in the bay and with renewed interest in restoring water quality and living resources. Since then, a primary management goal has been restoration of the bay through reduction of nutrient loads. According to recently-formulated water quality criteria (USEPA, 2008), the bay suffers from specific water quality impairments in three areas: dissolved oxygen, water clarity, and chlorophyll concentration. A set of mandatory Total Maximum Daily Loads (TMDLs) of nutrients from the watershed, designed to alleviate the impairments, is under development.

1.1. The Chesapeake Bay environmental model package

Predictive, mechanistic models have informed management actions since the inception of the CBP. The models have been continuously revised and improved to reflect new knowledge and to meet increasingly stringent demands on their capabilities. The present suite of management models is denoted as The Chesapeake Bay Environmental Model Package (CBEMP). The suite includes: an atmospheric deposition model which computes atmospheric nutrient loads to the watershed and water surface (Grimm and Lynch, 2004; Dennis et al., 2010), a watershed model which

* Corresponding author.
E-mail addresses: carl.f.cerco@usace.army.mil (C.F. Cerco), sung-chan.kim@usace.army.mil (S.-C. Kim), mark.r.noel@usace.army.mil (M.R. Noel).

0272-7714/$ – see front matter Published by Elsevier Ltd.
http://dx.doi.org/10.1016/j.ecss.2012.07.009

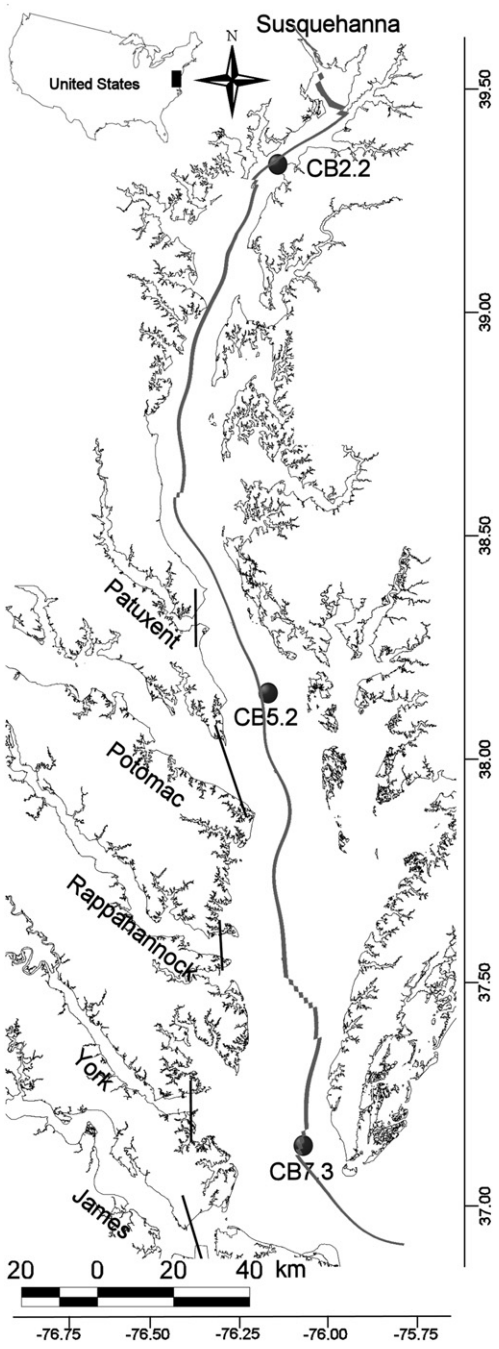

Fig. 1. The mainstem of Chesapeake Bay. The figure shows the axis for plotting longitudinal solids distribution and three stations for plotting time series. Transects for computing solids transport across the mouths of major tributaries are shown.

provides computations of runoff, nutrient loads, and solids loads (USEPA, 2010), a hydrodynamic model which computes transport processes (Johnson et al., 1993), and a eutrophication model which computes water quality and living resources (Cerco and Cole, 1993).

1.2. Management modeling of suspended solids

The disappearance of SAV is primarily attributed to increased light limitation (Kemp et al., 1983; Twilley et al., 1985) imposed by diminished water clarity and by epiphytes attached to SAV leaves and stems. Light is attenuated in the water column by particulate and dissolved organic matter and by inorganic particles (Gallegos, 2001). Epiphytic material is composed of periphyton and organic and inorganic particulate matter which associates with the periphyton to form a matrix of materials (Carter et al., 1985). Reduction of nutrients in the water column improves water clarity by limiting the production of phytoplankton and periphyton. In some regions of the bay system, however, light attenuation by inorganic solids is significant and SAV will not propagate without a reduction of both organic and inorganic material in the water column (Cerco and Moore, 2001). Consequently reduction of inorganic solids loads to the system may be a feasible management option to reduce light attenuation and promote production of SAV. Inorganic solids originate from multiple external sources. Their residence time in the water column is extensive due to continuous deposition and resuspension. A realistic predictive model must account for resuspension as well as external loads and transport. We report here on a management model of suspended solids in Chesapeake Bay that includes both organic and inorganic particulate material. Our model is distinctive in that a mechanistic model of inorganic solids transport is incorporated into the eutrophication portion of the CBEMP. Our motivation is that biological processes, as well as physical processes, influence the formation and transport of inorganic solids. Consequently, processes which determine transport and fate of inorganic solids must be considered simultaneously with the suite of eutrophication processes and living resources. We focus on model results in the mainstem of the bay and in smaller tributaries and embayments which adjoin it (Fig. 1). Complete results, including the major western tributaries, may be found in Cerco et al. (2010).

2. Material and methods

2.1. Model basics

The computation of inorganic suspended solids (ISS) requires interactions of multiple models and algorithms (Fig. 2). Loads originate in the watershed and as bank erosion. Transport processes are determined by the CH3D-WES hydrodynamic model (Johnson et al., 1993). Volumetric flows and vertical diffusivities are output from CH3D-WES, on an hourly basis, and stored as a data set for repeated use by the CE-QUAL-ICM eutrophication model (Cerco and Cole, 1993; Cerco and Meyers, 2000). For computation of inorganic solids, current-generated bottom shear stresses were added to the information output by the hydrodynamic model. Wave-generated bottom stresses were computed by a separate wind-wave model and combined into a single data set of bottom skin friction (Harris et al., in press). Wave action also

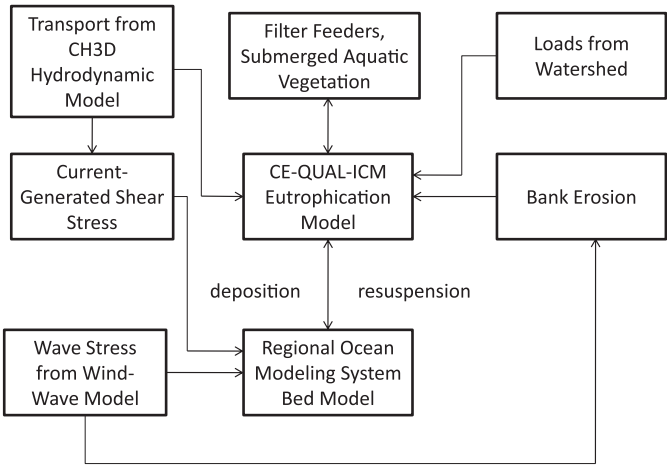

Fig. 2. Schematic of the inorganic suspended solids model.

determines the time course of bank erosion (Cerco et al., 2010). A multi-layer sediment bed model was adapted from the Regional Ocean Modeling System (ROMS, Warner et al., 2008). The sediment bed exchanges material with the model of the water column via the actions of deposition and resuspension. Deposition and resuspension are also affected by the actions of SAV and bivalve filter feeders (Cerco and Moore, 2001; Cerco and Noel, 2007), as calculated by sub-models within the eutrophication model. Suspended solids concentrations are converted to light attenuation using the algorithms of Gallegos et al. (2011). The model runs used for development and exploration, and presented here, cover a ten-year time period, 1991–2000. Additional descriptions of model features are described below. Complete details may be found in Cerco et al. (2010).

2.2. The hydrodynamic model

CH3D-WES is a three-dimensional hydrodynamic model which computes salinity, surface elevation, velocity, diffusivity, and bottom shear stress. Solutions are obtained via finite-difference approximations to the equations of continuity, motion, and mass conservation. For this application, the model operates on a computational grid of 50,000 elements which extends from the mouth of the bay to the heads of tide of the bay and major tributaries. A non-orthogonal curvilinear coordinate system is used in the horizontal plane. A Z-plane coordinate system, in which the number of layers varies according to local depth, is used in the vertical. The grid incorporates 11,000 surface cells ($\approx$1 km $\times$ 1 km) and 1–19 layers. Thickness of all layers is constant (1.5 m) except for the surface layer (2.14 m thick at mean tide) which varies according to tidal and wind forcing. The integration time step is 90 s.

2.3. The model of the water column

Eutrophication processes are computed by the CE-QUAL-ICM (or simply ICM) eutrophication model. ICM is an unstructured finite-volume model designed to accept transport information from a variety of hydrodynamic models. For this application, volumes on the unstructured ICM grid correspond exactly to cells on the structured CH3D grid. The eutrophication processes have been described elsewhere (Cerco and Cole, 1993; Cerco and Meyers, 2000). We focus here on new additions for modeling ISS. Inorganic solids are modeled as four size classes: fine clay, clay, silt, and sand. The size classes are distinguished by the magnitude of their settling velocity rather than strict adherence to actual diameter. Each class is represented by the mass-conservation equation which represents all ICM state variables:

$$\frac{\delta V_j C_j}{\delta t} = \sum_{k=1}^{n} Q_k C_k + \sum_{k=1}^{n} A_k D_k \frac{\delta C}{\delta x_k} + \sum S_j \tag{1}$$

where V_j = volume of jth control volume (m^3), C_j = concentration in jth control volume (g m^{-3}), Q_k = volumetric flow across flow face k of jth control volume (m^3 s^{-1}), C_k = concentration in flow across flow face k (g m^{-3}), A_k = area of flow face k (m^2), D_k = diffusion coefficient at flow face k (m^2 s^{-1}), n = number of flow faces attached to jth control volume, S_j = external loads and kinetic sources and sinks in jth control volume (g s^{-1}), and t, x = temporal and spatial coordinates. Solution to the mass-conservation equation is via the finite-difference method using the QUICKEST algorithm (Leonard, 1979) in the horizontal plane and a Crank–Nicolson scheme in the vertical dimension. Integration time step is 5 min. The only internal source/sink for inorganic solids in the water column is settling. For model cells which interface with the sediment bed, resuspension and deposition provide additional source/sink terms which are described below.

2.4. Fluxes at the sediment–water interface

Representations of erosion and deposition were selected from formulations previously applied to Chesapeake Bay. Deposition is modeled as a continuous process utilizing the settling velocity through the water column, as outlined by Sanford and Halka (1993):

$$D_i = Ws_i \cdot C_i \tag{2}$$

where D_i = deposition rate of solids size class i (g m^{-2} s^{-1}), Ws_i = settling velocity of solids size class i (m s^{-1}), and C_i = concentration of solids size class i (g m^{-3}).

The representation of erosion from a bed consisting of mixed sediment classes is a complex problem. The characteristics of the mixture differ from the characteristics of the individual fractions and, furthermore, evolve as the mixture ages and compacts. The formulation for clay and silt is adopted from Sanford and Maa (2001):

$$E(z,t) = M(z) \cdot [\tau_b(t) - \tau_c(z)] \tag{3}$$

where M = erosion rate per unit of excess shear stress (kg m^{-2} s^{-2} P^{-1}), τ_b = applied shear stress (P), τ_c = critical shear stress for erosion (P), z = depth into sediments (m), and t = time coordinate (s).

The formulation allows for erosion rate and critical shear stress to vary with depth into the sediments. Implementation of this scheme was infeasible on a system-wide scale. Instead, the model relies on two features to limit erosion under the application of continuous excess stress: 1) The quantity eroded during any time step is limited to the amount in an "active" sediment layer; and 2) The bed armors. That is, readily eroded materials are lost, leaving resistant materials behind. Equation (3) considers erosion and critical shear stress for a sediment mixture. In the model, M and τ_c are specified for individual classes of clay and silt.

The erosion of sand is considered differently than clays and silt and follows Harris and Wiberg (2001). The model calculates sand erosion as the product of a near-bed reference concentration, Ca, and settling velocity:

$$E = Ca \cdot Ws \tag{4}$$

In the Harris and Wiberg formulations, Ca is dimensionless (actually cm^3 cm^{-3}). For use in the model, E as calculated above is multiplied by ρ_s, the density of sand, and appropriate units conversions are conducted. The reader is referred to Harris and Wiberg (2001) for details of computing Ca.

2.5. The bed model

A suspended solids model which includes resuspension must incorporate a sediment bed model. The bed model for this study was adapted from the Regional Ocean Modeling System (ROMS). The ROMS bed model (Warner et al., 2008) consists of a fixed number of bed layers. The thickness and content of each layer are subject to change as material moves between the bed and the water column. An "active" layer is calculated at the sediment–water interface. Erosion during any model time step is restricted to the sediment mass in the active layer plus the amount deposited during the time step. The code was obtained from the ROMS web site (http://www.myroms.org/) and merged with the ICM code. Appropriate

modifications were made to incorporate the selected formulations for erosion and deposition and to ensure dimensional consistency.

The suspended solids model requires a set of initial conditions in the bed. The primary requirement is for bed fractions, by volume, for each solids class. These fractions are required for each bed layer in each bed cell, which correspond in number (11,000) and extent (1 km × 1 km) to model surface cells. Although guidelines exist, comprehensive quantitative data for initializing the model is not available. We arrived at a procedure in which initial conditions for a major calibration run or scenario were developed during a "spin-up" run. The procedure consisted of five steps: 1) The initial bed for the spin-up consists of seven layers, each one cm thick; 2) Set conditions in all cells and layers to the following volume fractions: fine clay (10%), clay (10%), silt (30%), sand (50%); 3) Run the model for five years using typical hydrodynamics, boundary conditions, and loadings; 4) Save the conditions in the bed at the end of the spin-up run; 5) Use this bed as the initial condition for the major calibration run or scenario. The bed thus-developed was predominantly sand with sporadic deposits of clay and silt (Cerco et al., 2010). The sandy bottom is an appropriate representation of the lower half of the bay and of the shoals in the upper bay although the observed predominance of clay in the upper-bay channel (Nichols et al., 1991; Halka, 2005) is not well-represented. Determination of initial bed conditions warrants additional attention in future model developments. Improved results might be obtained by initializing the model with a bed that approximately represents observations without attempting to resolve individual cells.

2.6. Waves and bottom shear stress

Bottom shear stress is the principal forcing factor that produces sediment resuspension. Throughout most of the bay system, bottom shear stress is generated by currents above the bed. Currents are computed by CH3D-WES and the resulting shear stress is computed as well, as one of the boundary conditions in the equations of motion. For some shallow regions of the bay, however, shear stress exerted by surface waves is significant relative to current-generated shear stress. Waves are not computed by CH3D-WES and, consequently, an independent wave model is necessary. The Young and Verhagen (1996) model for fetch- and depth-limited waves is employed. The model computes non-dimensional wave energy, ε, and frequency, ν, as a function of non-dimensional fetch, χ, and depth, δ. Wind velocity over the bay was obtained through interpolation of observations at five locations. Fetch was determined for each model surface cell for 16 directional bins (each 22.5°). These were used to determine wave properties at hourly intervals for the model application period.

The procedure for combining shear stress from currents and waves and for calculating skin friction is described by Harris et al. (in press). Four tasks are required: 1) Characterize sediment grain size throughout the model grid; 2) Obtain wave properties (from wave model) and current velocities (from CH3D-WES hydrodynamic model; 3) Estimate bed roughness; 4) Calculate combined wave-current bed stress and skin-friction shear stress. Note that the skin friction, which is used in sediment resuspension, is less than the total shear stress exerted on the bed.

The computed bottom shear stresses were compared to reported values from multiple locations and time intervals. In the upper bay, observations over several tidal cycles indicated peak bottom shear stresses between 1 and 2 dyne cm^{-2} (Sanford et al., 1991). Peak model values were of equivalent magnitude although the model showed a larger range since the simulation period exceeded the recording interval and represented a greater variety of forcing functions. Two independent studies were available from the lower bay. The first indicated peak current-generated bottom shear stresses were between 0.1 and 1 Pa (Wright et al., 1992). The model reflected these values well. The second study presented friction velocity, u^*. Observed values ranged between 0 and 2 cm s^{-1} (Fugate and Friedrichs, 2002) and this range was replicated in the model. Overall, the model bottom shear stresses reflected the magnitude of the observations in multiple locations in the bay system and formed a suitable basis for the sediment resuspension algorithms.

2.7. Parameter summary

A comprehensive, system-wide set of measurements to parameterize the suspended solids model did not exist although guidelines and measurements were available. Parameter evaluation was a recursive process in which an initial parameter set was refined based on judgment and quantitative evaluation of model performance. More than 400 calibration runs were performed to evaluate the complete ICM parameter set. Many of these were oriented toward calibration of the suspended solids model. Spatial variation was considered by assigning parameters into broad systems such as "mainstem bay" or "Potomac River." In the end, one universal parameter set was adopted (Table 1) which provided reasonable results systemwide.

The settling velocity employed for sand was much less than the velocity computed by Stokes law. The lesser velocity was determined, in part, to avoid the computation of negative sand or the alternative of unfeasible, short, model time steps. The role of sand in the model is primarily to armor the bed. Realistic computation of sand transport requires consideration of bedloads. The complexity of realistic sand computation was considered unnecessary in view of our focus on fine, suspended material which contributes to light attenuation.

2.8. Particulate organic matter

Earlier model versions (e.g. Cerco et al., 2004) employed a single class of ISS and did not include resuspension. Instead, the model relied on the concept of "retarded" or "net" settling. This net settling velocity represented the long-term difference between settling and resuspension and was typically much less than settling velocity in the water column. Once a particle settled to the bed, it stayed there. The present model retains the concept of net settling of particulate organic matter into the bed sediments, to facilitate interaction with the sediment diagenesis model (DiToro, 2001). Several lines of evidence indicate that net settling should be less in shallow littoral

Table 1
Suspended solids model parameter summary. Settling velocity for organic solids indicates transport through the water column. Net settling velocity describes deposition to bottom sediments. D is depth of the water column. (−) indicates not applicable.

	Fine clay	Clay	Silt	Sand	Organic solids
Settling velocity (μm s^{-1})	12	30	100	1000	11.6
Critical shear stress for erosion (P)	0.03	0.03	0.03	2	(−)
Erosion rate per unit of excess shear stress (g m^{-2} s^{-1} P^{-1})	1	1	1	(−)	(−)
Net settling velocity (μm s^{-1})	(−)	(−)	(−)	(−)	0.116, $D < 9.8$ m 2.32, $9.8 < D < 23.5$ 11.6, $D > 23.5$ m

areas and greater in deep channels. In an analysis of the Patuxent Estuary, Testa and Kemp (2008) found that lateral transport of particulate organic carbon (POC) to the central channel from adjacent shallow waters was required to meet bottom water respiratory demands. A similar analysis of the mesohaline Chesapeake Bay (Kemp et al., 1997) found that the littoral zones were net autotrophic (oxygen production exceeds consumption) while the main channel was net heterotrophic (oxygen consumption exceeds production). The difference between production and consumption suggests the transport of organic matter from the shoals to the channel. To reproduce the observed phenomena, we varied net settling according to depth (Table 1) with smaller values in shallow water to reflect the influence of wind-generated waves on resuspension. As a result of the spatially-varying deposition rate, computed channel sediments were carbon-rich compared to shoal regions.

2.9. Living-resource feedbacks

Transport and fate of ISS were incorporated into ICM to allow for feedback effects between ISS and living resources including bivalve filter feeders and SAV. The potential for filter feeders to remove solids from the water column is well known (Cohen et al., 1984; Caraco et al., 2006) and an earlier version of this model examined the use of oysters to remediate poor water clarity (Cerco and Noel, 2007). Oysters have little influence on water clarity at their present depleted population, however, and an examination of oyster restoration in concert with the latest model formulations has not yet been conducted. Oysters, at their present population levels, are included in the present model but their effect is negligible.

The ability of SAV to damp suspended solids has been observed in multiple environments (e.g. Ward et al., 1984; Carter et al., 1988; James et al., 2004). Damping arises from suppression of waves, anchoring of bottom sediments, and filtering of the water column. Relationships to quantify the effects of SAV on solids have been proposed but their utility in the model is limited due to inconsistencies between state variables, forcing functions, spatial and temporal scales. For the model, an approach was taken in which the presence of SAV damps bottom shear stress:

$$\frac{\tau_{sav}}{\tau} = \exp^{-k\cdot \mathrm{DEN}} \tag{5}$$

where τ_{sav} = shear stress as affected by SAV ($m^2\ s^{-2}$), τ = shear stress on non-vegetated bottom ($m^2\ s^{-2}$), DEN = SAV density averaged over SAV cell area (g C m^{-2}), and k = empirical constant which relates shear stress to density ($m^2\ g^{-1}$ C).

Model experiments indicate that $k = 0.015\ m^2\ g^{-1}$ C reduces suspended solids 1–2 g m^{-3} in SAV beds. The value $k = 0.1\ m^2\ g^{-1}$ C reduces suspended solids 5–10 g m^{-3}. Caution is necessary in evaluating the constant, however, since solids attenuation in SAV beds can influence the overall suspended solids calibration of the model. The value $k = 0.015$ was adopted for the model calibration and considered reflective of current SAV densities.

2.10. The data base

The CBP conducts a monthly monitoring program at more than 40 stations in the mainstem of Chesapeake Bay. Samples for laboratory analysis are routinely collected 1 m below the surface, 1 m above the bottom, and above and below the pycnocline. Deviations from routine occur according to local conditions and sampling agency. The prevalent analysis available for comparison with the model is total suspended solids (TSS). (Details of the sampling program, descriptions of analytical methods, and observations can be obtained at the CBP data hub: http://www.chesapeakebay.net/data_waterquality.aspx). No single model component compares directly with the prevalent observed quantity. For comparison with the data, model fine clay, clay, silt, and sand are summed into model ISS. Multiple forms of particulate organic matter, including phytoplankton, zooplankton, and detritus are modeled, all quantified as carbon. These particulate organic carbon forms are summed and multiplied by 2.5 to convert to organic suspended solids (OSS). The conversion factor is based on the assumption that organic matter is composed in the ratio CH_2O. Model ISS and OSS are finally summed to obtain model TSS for comparison with the observations. Volatile suspended solids (VSS) exist sporadically in the data base, primarily in the years 2001–2005. Although these years are outside the application period, the VSS observations provide an indication of the OSS, based on the analogy between solids lost on ignition and organic matter (APHA, 2005).

Twenty-one stations along the channel from mouth to head (Fig. 1) are selected for presentation of the longitudinal distribution of suspended solids. Three stations, one each in the upper, middle, and lower bay, are selected for presentation of time series (Fig. 1). In view of the importance of suspended solids in light attenuation, we emphasize surface samples which are in the photic zone and diminish light available to phytoplankton and SAV.

2.11. Suspended solids loads

2.11.1. Tributary loads

Solids loads from major tributaries were input at the tributary head-of-tide on a daily basis. These loads were provided by Phase 5.3.0 of the CBP Watershed Model (WSM, USEPA, 2010). The WSM provided loads of clay, silt, and sand. Silt and sand were routed into corresponding model components. WSM clay was sub-divided into two forms, fine clay and clay. The fine clay variable was required to provide a solids component that settled slowly and remained in suspension at great distances from loading sources. No guidance was available to specify the split into fine clay and clay. A constant concentration of 4 g m^{-3} fine clay in runoff was developed during the model calibration phase. The excess of WSM clay above 4 g m^{-3} was routed into the model clay variable.

The WSM contained no component which corresponded to organic solids or organic carbon. The model did consider particulate nitrogen. WSM particulate nitrogen was multiplied by a ratio based on observations at the tributary head of tide to obtain POC which was loaded to the model as detritus. The ratio varied locally in the range 6–8 g C g^{-1} N. For analysis of loads and comparison with observations, POC was converted to OSS as previously mentioned.

The WSM provides loads under existing conditions and under the management scenario denoted as the “allocation load.” The allocation load scenario repeats the 1991–2000 hydrology but substitutes loads determined to eliminate water quality impairments, largely through controls on nitrogen and phosphorus. Reductions in solids loads co-occur with controls on nutrients because a large fraction of nonpoint-source phosphorus loads is attached to suspended solids. The co-occurring solids load reductions are considered in the evaluation of water clarity goal attainment. For the allocation run, a new equilibrium sediment bed was computed according to the procedure described in Section 2.5, based on watershed solids loads under allocation conditions.

2.11.2. Distributed loads

Solids loads along the shoreline of the bay below the head of tide were provided by the WSM on a daily basis. Distributed loads were routed into model cells which adjoin the shoreline. Loads to each cell were determined by characteristics of the local watershed and by drainage area adjacent to the cell. WSM solids and particulate nitrogen loads were routed into WQM components as

described above. Distributed loads were provided for existing conditions and for the allocation load.

2.11.3. Bankloads

Quantifying solids loads from bank erosion requires two fundamental calculations. First, the volume of sediment lost from erosion is calculated based on shoreline length, rate of shoreline retreat, and bank height. Sediment volume is converted to sediment mass through multiplication by bulk density. More than 250,000 shoreline-normal transects were available to determine the rate of shoreline retreat. For the load calculations, the two most recent shorelines in each analyzed reach or section were utilized. For most areas, the two most recent shorelines dated from *circa* 1940 and *circa* 1990, though intervals shorter and longer than 50 years occurred. Shoreline characteristics, notably the presence of protective structures, were considered in the load computation. When necessary, missing information (recession rate, presence of structures, bulk density) was derived from adjacent shoreline reaches or from regional average characteristics.

The bankload study resulted in decadal-average mass erosion rates per unit shoreline length throughout the bay system. A geographic information system (GIS) was employed to merge three key pieces of information: mass erosion rates, shoreline length, and the CBEMP computational grid. Shoreline length was assigned to each cell adjoining the shore and the mass loading to each cell was computed. Decadal-average loads were partitioned into daily loads as follows: 1) Compute the total bankload to each cell for the application period (10 years * annual average load); 2) Compute the daily energy dissipated on the shoreline of each cell by wave action and inundation; 3) Sum the daily energy into total energy dissipated on the shoreline of each cell over the application period; 4) Assign daily loads according to the fraction of total energy dissipated on each day of the application period.

Daily energy dissipated was computed as a function of wavelength, period, and inundation height (Cerco et al., 2010):

$$E_t = \rho \cdot g \cdot \left[\frac{H^2}{4} + \Delta z^2\right] \cdot \frac{L}{2} \cdot \frac{D}{T} \quad (6)$$

where E_t = daily total energy exerted per unit wave crest width (J m^{-1}), H = wave height (m), Δz = inundation height above mean sea level (m), L = wavelength (m), T = wave period (s), D = daylength (86,400 s), ρ = density of water (kg m^{-3}), and g = gravitational acceleration (m s^{-2}). Occasionally the sea surface exhibits a "set down" due the local or remote wind effects. In the event of set down (negative Δz), the energy exerted by inundation was set to zero.

Bankloads were quantified as coarse and fine material. Coarse material was routed to the ICM sand variable. Fine material was split 60% clay and 40% silt. The present work considers no management actions to reduce bankloads although actions are available and under consideration.

Erosion from marshes located along the shorelines of the bay and tributaries was included in the estimation of bankloads. Substantial erosion also occurs in interior marshes, however, especially on the eastern shore of the bay (Kearney et al., 2002). Mass erosion rate from interior marshes, including organic matter, was calculated and combined with bankloads to the nearest model cell. Details of the procedure may be found in Cerco et al. (2010).

3. Results

3.1. Temporal and spatial distributions of suspended solids

Three stations are selected for presentation of time series (Fig. 1): CB2.2, in the upper bay, CB5.2, mid-way between the ocean boundary and the freshwater source, and CB7.3 in the lower bay. The pre-eminent features of the calculated time series at CB2.2 are solids concentrations in excess of 300 g m^{-3} (Fig. 3a) in late winter and spring. Concentrations of this magnitude are observed in runoff from the Susquehanna River (USGS, 2011) but few of the monthly surveys coincide with these brief excursions. The observations reflect the influence of runoff events with the highest solids concentrations observed in the winter months from November to April. High concentrations also occur associated with late-summer tropical storms (Chesapeake Research Consortium, 1976) but none are contained in our application period. Runoff events are evident in the model calculations at mid-bay (Fig. 3b) and mean concentrations in the months from February to April are distinctly higher than the remainder of the year. Events are more difficult to identify in the observations, however, and no monthly or seasonal pattern is distinguishable. Events are once again evident in the observations in the lower bay (Fig. 3c). The seasonality is different from the upper bay, however, and several of the highest concentrations are observed in June and July. The higher solids concentrations, compared to mid-bay, and the altered seasonality suggest the influence of meteorological events or other forcings beyond the mouth of the bay, outside the model domain. Concentration boundaries at the edge of the grid are specified to reflect observations but gaps exist in the data and effects from propagation of waves generated outside the domain cannot be considered.

For comparison purposes, model results and observations along the bay axis are combined into seasonal averages. We examine here (Fig. 4) results from three SAV growing seasons (April–October). These months represent the period when water clarity is a critical criterion. The seasons are selected from years in which winter–spring runoff is low, average, and high relative to the ten-year application period. The bay exhibits a classic turbidity maximum (Schubel, 1968; Sanford et al., 2001) at the head of the salt intrusion, roughly 280 km from the mouth. Both observations and model indicate the maximum is weaker in the low-flow year, when loading at the fall line is less and density-driven residual circulation is weak. The observed solids minimum is in mid-bay, between km 100 and 200, and varies little from year to year. Chesapeake Bay exhibits a secondary, persistent, solids maximum roughly 60 km from the mouth. The origin of this feature is unclear. This maximum has not attracted investigative attention as with the classic up-estuary turbidity maximum. The secondary solids maximum is not captured in the model, suggesting its causal mechanisms are not incorporated in the model framework. The time series near the bay mouth suggested the influence of actions outside the model domain. These actions, for example the presence of ocean swells, may exert influence the creation of the secondary solids maximum.

The turbidity maximum is prominent in a view of average computed ISS over the surface of the bay (Fig. 5a). The figure also reveals high solids concentrations near sources in several tributaries situated on the middle, eastern, shore of the bay. Minimal ISS concentrations occur in the lower bay, removed from tributary loads and the oceanic boundary condition, and in several upper eastern-shore tributaries. A similar illustration of model OSS (Fig. 5b) indicates the Susquehanna loading source and OSS concentrated in the turbidity maximum. The highest concentrations are exhibited in the middle, eastern-shore, tributaries and in the central bay. In both regions, the elevated OSS concentrations originate with internal production, supplemented, along the eastern shore, by internal marsh erosion.

Minimal OSS concentrations are computed in small embayments and tributaries situated primarily along the eastern shore but also near the mouth of the York River. These concentrations indicate the operation of positive feedback mechanisms (Fig. 6).

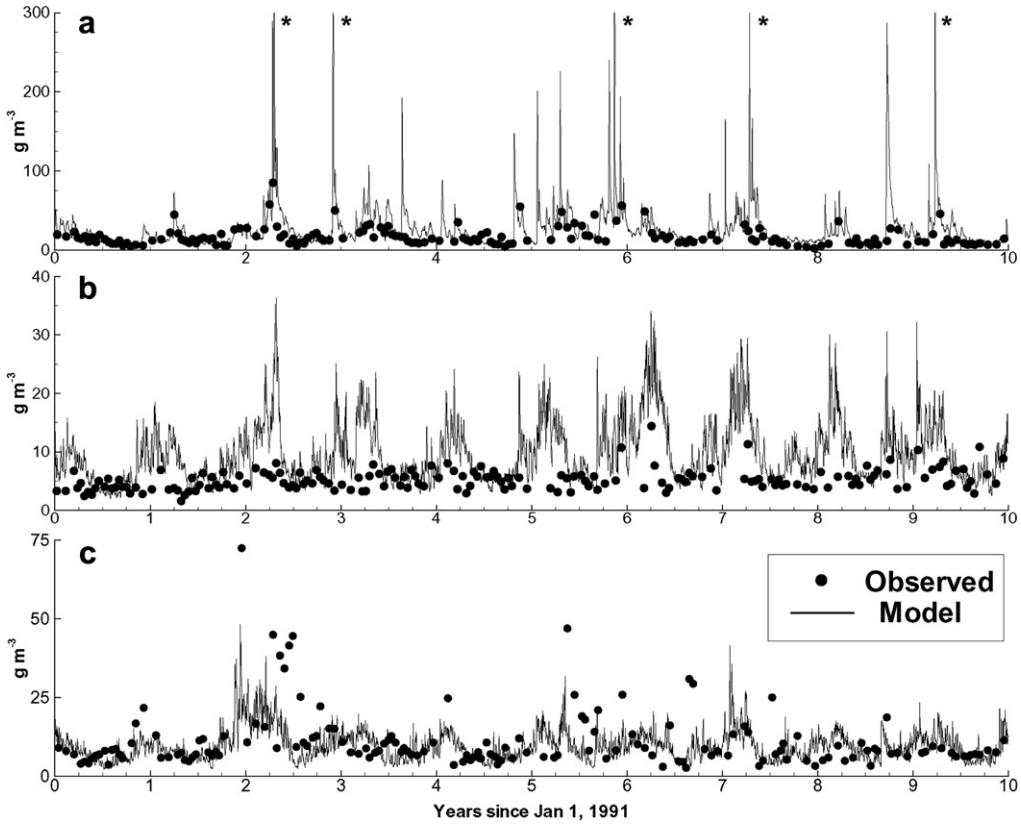

Fig. 3. Computed and observed surface total suspended solids at three locations in Chesapeake Bay: a) Station CB2.2 in the upper bay; b) Station CB5.2 in the middle bay; and c) Station CB7.3 in the lower bay.

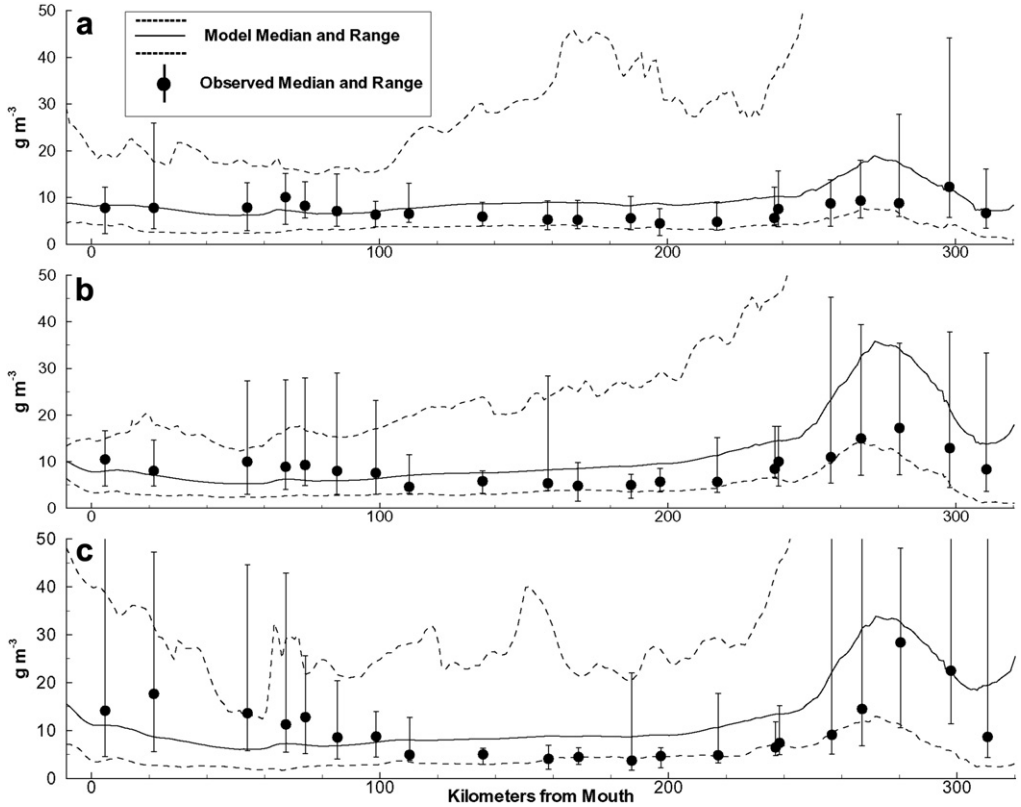

Fig. 4. Computed and observed surface total suspended solids along the axis of Chesapeake Bay. Results are shown for April–October of three years with: a) low winter–spring runoff; b) moderate winter–spring runoff; and c) high winter–spring runoff.

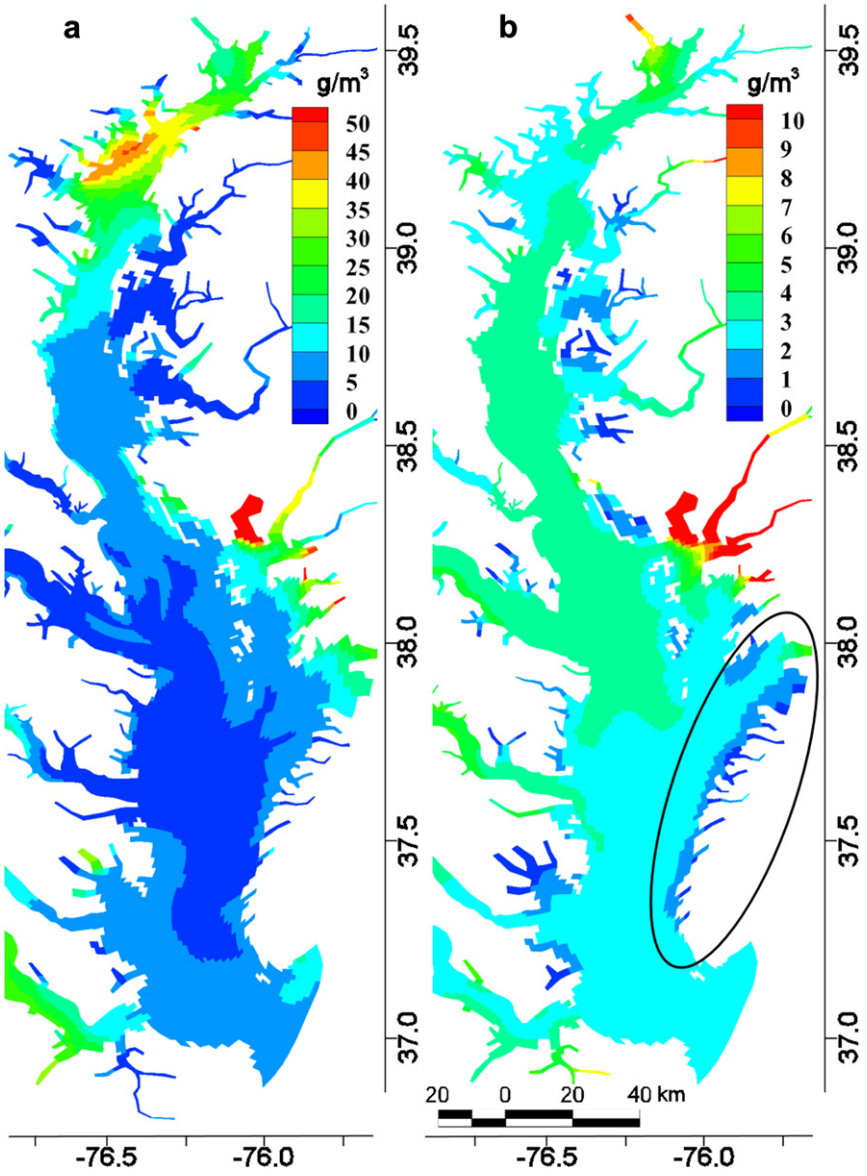

Fig. 5. Computed: a) inorganic suspended solids; and b) organic suspended solids in the surface waters of the mainstem Chesapeake Bay. Concentrations are arithmetic averages over the submerged aquatic vegetation growing season, April–October for a year of average hydrology (1994). Several lower eastern shore embayments which benefit from a positive feedback mechanism between submerged aquatic vegetation and reduced production of organic solids are circled.

SAV is present in these shallow systems and damps sediment resuspension. Less resuspension leads to increased transparency and stimulates production of SAV and of benthic algae (Cerco and Seitzinger, 1997). The algae retain nutrients in the sediments and discourage phytoplankton production. Lower production results in lower OSS and increased transparency.

3.2. Solids budgets

Numerous sediment budgets for Chesapeake Bay and its subsystems have been compiled. The budgets rely on a variety of methods and accounting. Although the elements of the budgets quantitatively differ, a consistent picture of the sediment budget can be derived. The bay is a depositional environment. Net deposition is evident over geological time scales (the bay is a drowned river) and has been quantified by comparison of bathymetric measures collected over a century (Hobbs et al., 1992). Solids sources include the watershed above the fall-line, the watershed adjacent to the bay, bank and marsh erosion, the coastal waters outside the bay mouth, and biogenic production. The watershed above the fall line is a major source of fine grained material while the preponderance of oceanic loading is in the form of sand (Hobbs et al., 1992) although fine-grained oceanic sediments are deposited in the bay as well (Skrabal, 1991). A large portion of the watershed load is trapped in the upper-bay turbidity maximum (Schubel, 1968) so that bankloads and internal production are predominant loading sources in the middle and lower bay (Biggs, 1970; Schubel and Carter, 1976; Marcus and Kearney, 1991). The turbidity maxima in the western tributaries trap solids from their watersheds so that the lower portions of the western tributaries are solids sinks relative to the mainstem bay (Schubel and Carter, 1976; Officer and Nichols, 1980).

Quantitative budgets often focus on fine-grained material since this fraction contributes to light attenuation and other negative effects. Construction of a meaningful budget that includes sand is difficult since sand transport is predominantly as bedload (Hobbs et al., 1992) which is difficult to measure and quantify. Absent computation of bedload, our computation of sand transport as

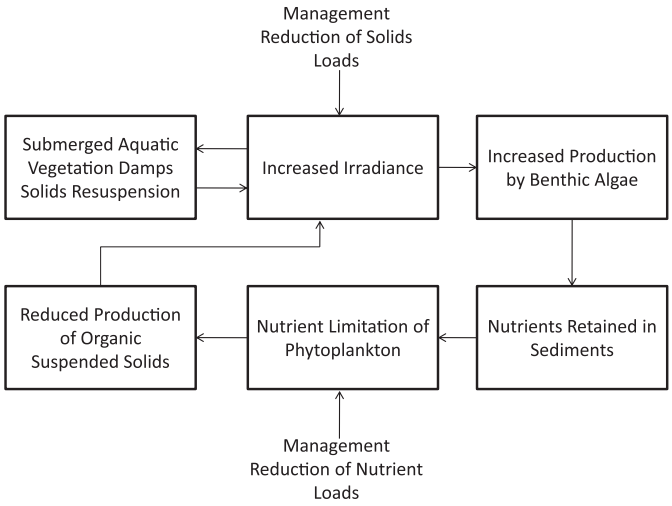

Fig. 6. A positive feedback mechanism in which the presence of submerged aquatic vegetation leads to reduced production of organic suspended solids. The mechanism is enhanced by management actions to reduce solids loads or nutrient loads.

suspended load represents only a fraction of total transport. Our budgets include model fine clay, clay, silt, and OSS (estimated as 2.5 × POC). Loads from the Susquehanna, distributed loads, and bankloads are readily obtained from the model input files. These were first summed into individual years and then averaged over the model application period. Exchange between the mainstem and major western tributaries was calculated at transects near the mouth of each tributary (Fig. 1). A "transport flux" feature of the ICM model computed transport of each solids component at each model time step. Following the procedure for loads, the fluxes were summed for each model year and then averaged across all years. An identical procedure was used to compute exchange between the bay and adjacent coastal waters. Internal solids production was taken as the net primary production (NPP, Cerco and Noel, 2004) of carbon and converted to OSS. NPP, as g C m^{-2} d^{-1}, for each model cell was multiplied by cell area, summed over each year, and then summed over the cells representing the mainstem bay. Finally, the bay-wide summary for each year was averaged for comparison with the loads and fluxes.

Under calibration conditions (Table 2), the greatest source of fine-grained ISS to the bay is from bankloads, followed by the Susquehanna River and then the ocean. Four of the major western tributaries import sediment from the bay. Only in the James does sufficient clay pass through the local turbidity maximum to provide a net solids source to the bay. The largest source of material to the bay, however, is from internal production. Internal production of organic solids nearly equals the external loading of inorganic solids. A significant difference between the two sources is that ISS are effectively conservative while OSS are subject to breakdown by a host of biotic processes operating on multiple time scales. Still, the VSS observations indicate that, on average, 36% of the TSS in the mainstem bay consists of organic matter.

Under allocation conditions (Table 3), bankloads and internal production retain their roles as the leading source of ISS and the leading source of TSS, respectively. For this simulation, controls on bankloads were not considered although environmentally benevolent controls are available, are being promoted, and can be considered in future scenarios. Solids from the second largest source, the Susquehanna, decline by 65% under allocation conditions and internal production declines by 33%. The decrease in internal production represents the greatest decline in terms of mass loading. The declines in solids loading are countered, to an extent by an increase in ISS imported from the ocean and a reduction in OSS exported. Overall, the total mass loading to the bay of all solids forms declines by 25%.

3.3. Altered solids distribution due to allocation loads

Changes in ISS due to load reductions occur primarily in the upper half of the bay (Fig. 7a). Virtually no change occurs in the lower half, far removed from controllable sources in the watershed. The largest reductions in OSS, in magnitude, occur near loading sources but these are of limited spatial extent (Fig. 7b). Smaller reductions, but of baywide extent, occur as a result of nutrient limitations to internal production.

4. Discussion

A primary goal of our modeling activity was to incorporate a mechanistic suspended solids model into an eutrophication model, in order to represent biotic influences on solids processes. Results of this study indicate the importance of combining the heretofore disparate model activities. The largest computed source of solids to the mainstem Chesapeake Bay is internal production. The spatial distribution of this source and the reaction to management controls cannot be considered in a model which considers only physical processes and ISS. A second biotic interaction which figures in our computation is the damping of resuspension by SAV although our representation of the process is crude. An ideal model package would combine interactions between hydrodynamics, eutrophication processes, and suspended solids simultaneously although the computational demands would be great and the calibration process extensive. Our combined model

Table 2
Average annual solids budget (tonnes) for the mainstem of Chesapeake Bay based on the years 1991–2000. Negative numbers indicate a loss of solids from the bay.

	Fine clay	Clay	Silt	VSS	Total
Susquehanna	123,754	979,567	139,039	391,820	1,634,180
Local Watershed	13,346	119,363	172,707	72,421	377,837
Bankloads	615,447	791,395	843,024	303,367	2,553,233
Patuxent	−11,104	−9242	−3771	9658	−14,458
Potomac	−26,949	−26,500	−17,956	80,096	8690
Rappahannock	−24,856	−17,848	−17,402	9648	−50,458
York	−8278	−20,374	−49,006	2114	−75,544
James	45,158	126,797	−77,026	54,979	149,908
Bay Mouth	152,026	173,464	651,919	−173,331	804,078
Internal Production				4,905,100	4,905,100
Total	878,544	2,116,622	1,641,528	5,655,871	10,292,565

Table 3
Average annual solids budget (tonnes) for the mainstem of Chesapeake Bay based on allocation loads of nutrients and solids. Hydrology from the years 1991 to 2000. Bankloads are uncontrolled in this budget. Negative numbers indicate a loss of solids from the bay.

	Fine clay	Clay	Silt	VSS	Total
Susquehanna	93,170	201,213	52,474	226,054	572,911
Local Watershed	13,013	93,207	141,942	39,194	287,356
Bankloads	615,447	791,395	843,024	303,367	2,553,233
Patuxent	−9346	−5406	−3880	4762	−13,870
Potomac	−24,165	−12,610	−17,937	49,161	−5550
Rappahannock	−23,443	−13,923	−17,318	3258	−51,425
York	−8429	−19,666	−48,941	901	−76,135
James	36,666	91,258	−77,847	40,275	90,352
Bay Mouth	181,096	227,108	653,193	−24,683	1,036,714
Internal production				3,281,850	3,281,850
Total	874,010	1,352,577	1,524,710	3,924,138	7,675,435

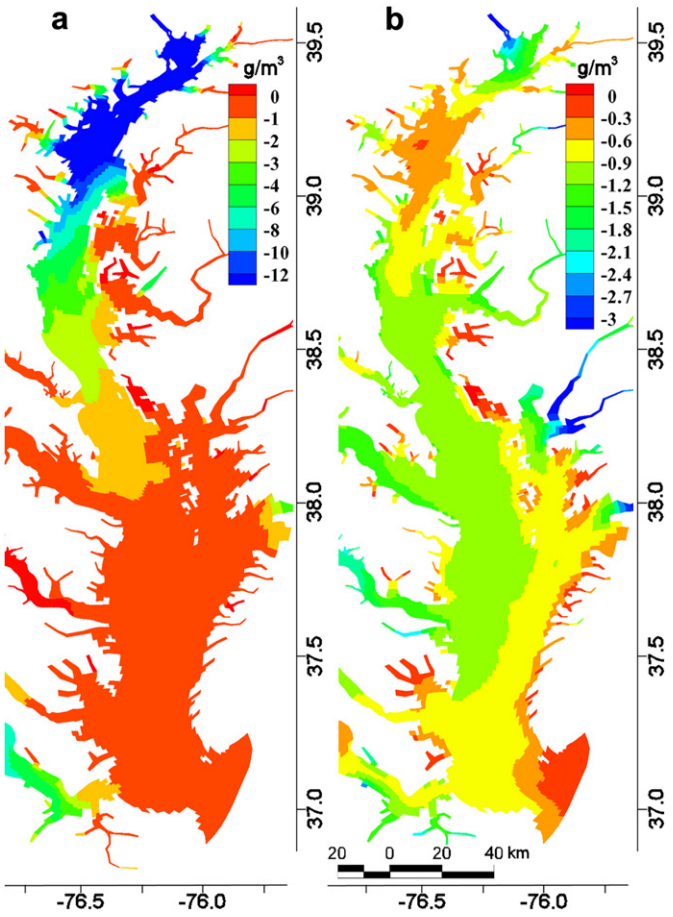

Fig. 7. Reductions in: a) inorganic suspended solids; and b) organic suspended solids computed to occur in surface waters of Chesapeake Bay as a result of reductions in nutrient and solids loads to meet Total Maximum Daily Load allocations. Concentrations are arithmetic averages over the submerged aquatic vegetation growing season, April–October, for a year of average hydrology (1994).

also incorporates feedbacks between bivalve filter feeders and suspended solids. At present these feedbacks are negligible although they were significant in the past (Newell, 1988) and may figure into future management actions (Cerco and Noel, 2007).

Our modeling process revealed an emergent property that acts to reduce suspended solids in shallow water. A positive feedback loop exists involving SAV, benthic algae, and phytoplankton. The combined actions of the SAV and the benthic algae reduce both solids production and solids resuspension. The potential of the loop to influence suspended solids requires a model representation of biotic interactions.

Our model solids budget attributes a major role to internal production. A summary of solids budgets for the bay and tributaries (Langland and Cronin, 2003) indicates inconsistent treatment of internal solids production. Budgets may consider internal production of POC by primary production, internal production of biogenic silica, both sources, or neither source. Explicit consideration of internal production by Biggs (1970) indicated it was a major solids source in the bay mid-section. Available observations indicate that VSS comprise a variable but significant fraction of TSS. Gallegos and Moore (2000) examined the VSS/TSS fraction in several bay tributaries and found values as high as 90% although the preponderance of the observations was in the range 10–30%. Our own analysis of the 2000–2005 data collected at our time series stations (Fig. 1) indicates mean VSS/TSS fractions ranging from 28% (CB2.2) to 55% (CB5.2) to 32% (CB7.3). Model mean values over the simulation period range from 15% to 30%. If we assume the 2000–2005 data characterize the 1991–2000 simulation period, then the modeled fraction is low. We cannot determine if this indicates that the model budget underestimates internal production or if the model sources and sinks of OSS are out of balance. The observations also indicate that the ratio 2.5 used to convert model POC to OSS is closer to 3.0 although revision of this ratio is not sufficient to reconcile the difference between the observed and computed organic fraction of TSS.

The field of suspended solids transport is under continuing development and is far from mature. The present model has reached its optimal state of development, however. In several regards, the model is ahead of our understanding and our observations, and indicates that our fundamental understanding of relevant processes must be strengthened. We have noted (Section 3.1) the existence of the lower bay suspended solids maximum which is not represented in the current model. The activity of the positive feedback loop (Section 3.1) is feasible and provocative but difficult to validate with existing observations. There are other processes, as well, such as the influence of phytoplankton on particle aggregation and settling (Passow, 2002; de la Rocha, 2006) which merit investigation and potential incorporation into the modeling process.

Guidelines for management indicated by our model are that control of solids loads from the watershed is effective in reducing solids concentrations near the discharge points. Nutrient controls limit internal solids production baywide. Our model also indicates that management actions to control solids will benefit from positive feedback mechanisms. As solids are reduced, promoting light availability to SAV and benthic primary producers, these organisms will act to reduce solids further, promoting additional available light.

Management interest in suspended solids is amplified in shallow water since littoral regions are the site of SAV production. Detailed modeling of these regions is limited in a baywide model, however, due to the limitations of grid representation and computational requirements. Until recently, modeling of littoral regions was also hampered by paucity of observations. A shallow water monitoring program is now a regular part of baywide monitoring (MDDNR, 2011; STAC, 2011). The next step in management modeling is to focus on shallow water with an appropriate grid and modeling approach.

5. Conclusions

Our approach to modeling suspended solids transport and fate is distinctive in that a mechanistic model of inorganic solids transport is combined with a model of eutrophication processes. Our motivation is that biological processes, as well as physical processes, influence the formation and transport of suspended solids. Quantification and parameterization of biological effects are challenging, however, and substantial investigations into processes and modeling are required beyond our own work. Our model is used to create solids budgets and to investigate management scenarios. Results indicate that:

1) Organic solids comprise a significant fraction, often a third or more, of total suspended solids in mainstem Chesapeake Bay. Internal production of organic solids is equivalent in magnitude to external loading of inorganic solids.
2) Scenario analysis indicates control of solids loads reduces solids concentration in the vicinity of the loading sources. Control of nutrient loads provides more widespread but lesser reductions in suspended solids.

Acknowledgments

This study was funded by the US Army Engineer District, Baltimore, and by the US Environmental Protection Agency Chesapeake Bay Program Office. Jeff Halka, of the Maryland Department of Natural Resources – Maryland Geological Survey, led the team which computed loads from bank and marsh erosion. Scott Hardaway, of the Virginia Institute of Marine Science, provided invaluable assistance in computing bankloads in the Virginia portion of the bay. The algorithms for combining current-generated and wave-generated bottom shear stresses were developed by Courtney Harris and J. Paul Rinehimer of the Virginia Institute of Marine Science.

References

American Public Health Association, 2005. In: Eaton, A., Clesceri, L., Rice, E., Greenberg, A. (Eds.), Standard Methods for the Examination of Water and Wastewater. American Public Health Association, Washington, DC.

Biggs, R., 1970. Sources and distribution of suspended sediment in northern Chesapeake Bay. Marine Geology 9, 187–201.

Caraco, N., Cole, J., Strayer, D., 2006. Top-down control from the bottom: regulation of eutrophication in a large river by benthic grazing. Limnology and Oceanography 51, 664–670.

Carter, V., Paschal, J., Bartwo, N., 1985. Distribution and Abundance of Submersed Aquatic Vegetation in the Tidal Potomac River Estuary, Maryland and Virginia, May 1978 to November 1981. U.S. Geological Survey Water Supply Paper 2234-A. United States Geological Survey, Alexandria, VA.

Carter, V., Barko, J., Godshalk, G., Rybicki, N., 1988. Effects of submersed macrophytes on water quality in the tidal Potomac River, Maryland. Journal of Freshwater Ecology 4 (4), 493–501.

Cerco, C., Cole, T., 1993. Three-dimensional eutrophication model of Chesapeake Bay. Journal of Environmental Engineering 119 (6), 1006–1025.

Cerco, C., Meyers, M., 2000. Tributary refinements to the Chesapeake Bay Model. Journal of Environmental Engineering 126 (2), 164–174.

Cerco, C., Moore, K., 2001. System-wide submerged aquatic vegetation model for Chesapeake Bay. Estuaries 24 (4), 522–534.

Cerco, C., Noel, M., 2004. Process-based primary production modeling in Chesapeake Bay. Marine Ecology Progress Series 282, 45–58.

Cerco, C., Noel, M., 2007. Can oyster restoration reverse cultural eutrophication in Chesapeake Bay? Estuaries and Coasts 30 (2), 331–343.

Cerco, C., Seitzinger, S., 1997. Measured and modeled effects of benthic algae on eutrophication in Indian River – Rehoboth Bay Delaware. Estuaries 20 (1), 231–248.

Cerco, C., Noel, M., Linker, L., 2004. Managing for water clarity in Chesapeake Bay. Journal of Environmental Engineering 130 (6), 631–642.

Cerco, C., Kim, S.-C., Noel, M., 2010. The 2010 Chesapeake Bay Eutrophication Model. A Report to the US Environmental Protection Agency Chesapeake Bay Program and to the US Army Engineer Baltimore District. Available from: http://www.chesapeakebay.net/publications/title/the_2010_chesapeake_bay_eutrophication_model1.

Chesapeake Research Consortium, 1976. In: Ruzecki, E., Schubel, J., Huggett, R., Anderson, A. (Eds.), The Effects of Tropical Storm Agnes on the Chesapeake Bay Estuarine System. CRC Publication 54. Johns Hopkins University Press, Baltimore, MD.

Cohen, R., Dresler, P., Phillips, E., Cory, R., 1984. The effect of the Asiatic clam, *Corbicula fluminea*, on phytoplankton of the Potomac River, Maryland. Limnology and Oceanography 29, 170–180.

de la Rocha, C., 2006. The biological pump. In: Elderfield, H. (Ed.), The Oceans and Marine Geochemistry. Elsevier, Amsterdam, pp. 84–107.

Dennis, R.L., Mathur, R., Pleim, J., Walker, J., 2010. Fate of ammonia emissions at the local and regional scale as simulated by the Community Multiscale Air Quality Model. Atmospheric Pollution Research 1 (4), 207–214.

DiToro, D., 2001. Sediment Flux Modeling. John Wiley and Sons, New York, 624 pp.

Fugate, D., Friedrichs, C., 2002. Determining concentration and fall velocity of estuarine particle populations using ADV, OBS, and LISST. Continental Shelf Research 22 (10), 1867–1886.

Gallegos, C., 2001. Calculating optical water quality targets to restore and protect submerged aquatic vegetation: overcoming problems in partitioning the diffuse attenuation coefficient for photosynthetically active radiation. Estuaries 24 (3), 381–397.

Gallegos, C., Moore, K., 2000. Factors contributing to water-column light attenuation. In: Batiuk, R. (Ed.), Submerged Aquatic Vegetation Water Quality and Habitat-Based Requirements and Restoration Targets. US Environmental Protection Agency Chesapeake Bay Program, Annapolis, MD, EPA 903-R-00-014, pp. 35–54.

Gallegos, C., Werdell, P., McClain, C., 2011. Long-term changes in light scattering in Chesapeake Bay inferred from Secchi depth, light attenuation, and remote sensing measurements. Journal of Geophysical Research 117, 1–19.

Grimm, J., Lynch, J., 2004. Enhanced wet deposition estimates using modeled precipitation inputs. Environmental Monitoring and Assessment 90, 243–268.

Hagy, J., Boynton, W., Keefe, C., Wood, K., 2004. Hypoxia in Chesapeake Bay, 1950–2001: long-term change in relation to nutrient loading and river flow. Estuaries 27 (4), 634–658.

Harris, C., Wiberg, P., 2001. A two-dimensional, time-dependent model of suspended sediment transport and bed re-working for continental shelves. Computers & Geosciences 27, 675–690.

Harris, C., Rinehimer, J., Kim, S.-C. Estimates of bed stresses within a model of Chesapeake Bay. In: Spaulding, M. (Ed.), Proceedings of the Twelfth International Conference on Estuarine and Coastal Modeling. American Society of Civil Engineers, Washington DC, in press.

Hobbs, C., Halka, J., Kerhin, R., Carron, M., 1992. Chesapeake Bay sediment budget. Journal of Coastal Research 8 (2), 292–300.

James, W., Barko, J., Butler, M., 2004. Shear stress and sediment resuspension in relation to submersed macrophyte biomass. Hydrobiologia 515, 181–191.

Johnson, B.H., Kim, K., Heath, R., Hsieh, B., Butler, L., 1993. Validation of a three-dimensional hydrodynamic model of Chesapeake Bay. Journal of Hydraulic Engineering 119, 2–20.

Kearney, M., Rogers, J., Townshend, E., Rizzo, E., Stutzer, D., Stevenson, J., Sundborg, K., 2002. Landsat imagery shows decline of coastal marshes in Chesapeake and Delaware Bays. Eos 83 (16), pp. 173, 177–178.

Kemp, W., Twilley, R., Stevenson, J., Boynton, W., Means, J., 1983. The decline of submerged vascular plants in the upper Chesapeake Bay: summary of results concerning possible causes. Marine Technology Science Journal 17, 78–89.

Kemp, W.M., Smith, E., DiPasquale, M., Boynton, W., 1997. Organic carbon balance and net ecosystem metabolism in Chesapeake Bay. Marine Ecology Progress Series 150, 229–248.

Kemp, W., Boynton, W., Adolf, J., Boesch, D., Boicourt, W., Brush, G., Cornwell, J., Fisher, T., Glibert, P., Hagy, J., Harding, L., Houde, E., Kimmel, D., Miller, W., Newell, R., Roman, M., Smith, E., Stevenson, J., 2005. Eutrophication of Chesapeake Bay: historical trends and ecological interactions. Marine Ecology Progress Series 303, 1–29.

Langland, M., Cronin, T., 2003. A Summary Report of Sediment Processes in Chesapeake Bay and Watershed. Water-Resources Investigations Report 03-4123. United States Geological Survey, New Cumberland, PA. Available from: http://pa.water.usgs.gov/reports/wrir03-4123.pdf.

Leonard, B., 1979. A stable and accurate convection modelling procedure based on quadratic upstream interpolation. Computer Methods in Applied Mechanics and Engineering 19, 59–98.

Marcus, W., Kearney, M., 1991. Upland and coastal sediment sources in a Chesapeake Bay Estuary. Annals of the Association of American Geographers 81 (3), 408–424.

Newell, R., 1988. Ecological changes in Chesapeake Bay: are they the result of overharvesting the American oyster (*Crassostrea virginica*)? In: Lynch, M., Krome, E. (Eds.), Understanding the Estuary – Advances in Chesapeake Bay Research. Chesapeake Research Consortium, Baltimore, MD, pp. 536–546 Publication 129.

Nichols, M., Kim, S., Brouwer, C., 1991. "Sediment Characterization of the Chesapeake Bay and Its Tributaries," NOAA National Estuarine Inventory. Virginia Institute of Marine Science, Gloucester Pt, VA.

Officer, C., Nichols, M., 1980. Box model application to a study of suspended sediment distribution and fluxes in partially-mixed estuaries. In: Kennedy, V. (Ed.), Estuarine Perspectives. Academic Press, New York, pp. 329–340.

Orth, R.J., Moore, K., 1983. Chesapeake Bay: an unprecedented decline in submerged aquatic vegetation. Science 222, 51–53.

Passow, U., 2002. Transparent exopolymer particles (TEP) in aquatic environments. Progress in Oceanography 55, 287–333.

Sanford, L., Panageotou, W., Halka, J., 1991. Tidal resuspension of sediments in northern Chesapeake Bay. Marine Geology 97 (1–2), 87–103.

Sanford, L., Halka, J., 1993. Assessing the paradigm of mutually exclusive erosion and deposition of mud, with examples from upper Chesapeake Bay. Marine Geology 114, 37–57.

Sanford, L., Maa, J., 2001. A unified erosion formula for fine sediments. Marine Geology 179, 9–23.

Sanford, L.P., Suttles, S.E., Halka, J.P., 2001. Reconsidering the physics of the Chesapeake Bay estuarine turbidity maximum. Estuaries 24 (5), 655–669.

Schubel, J., 1968. Turbidity maximum of the northern Chesapeake Bay. Science 161, 1013–1015.

Schubel, J., Carter, H., 1976. Suspended sediment budget for Chesapeake Bay. In: Wiley, M. (Ed.), Estuarine Processes, vol. II. Academic Press, New York, pp. 48–62.

Skrabal, S., 1991. Clay mineral distributions and source discrimination of upper quaternary sediments, lower Chesapeake Bay, Virginia. Estuaries 14 (1), 29–37.

Testa, J., Kemp, W.M., 2008. Variability of biogeochemical processes and physical transport in a partially stratified estuary: a box modeling analysis. Marine Ecology Progress Series 356, 63–79.

Twilley, R., Kemp, W., Staver, K., Stevenson, J., Boynton, W., 1985. Nutrient enrichment of estuarine submersed vascular plant communities. 1. Algal growth and effects on production of plants and associated communities. Marine Ecology Progress Series 23, 179–191.

United States Environmental Protection Agency, 2008. Ambient Water Quality Criteria for Dissolved Oxygen, Water Clarity and Chlorophyll a for the Chesapeake Bay and its Tidal Tributaries. EPA 903-R-08-001. Chesapeake Bay Program Office, Annapolis, MD. Available from: http://www.chesapeakebay.net/content/publications/cbp_47637.pdf.

United States Environmental Protection Agency, 2010. Chesapeake Bay Phase 5.3 Community Watershed Model. EPA Report 903S10002. Chesapeake Bay

Program Office, Annapolis, MD. Available from: http://www.chesapeakebay.net/model_phase5.aspx?menuitem=26169.
Warner, J., Sherwood, C., Signell, R., Harris, C., Arango, H., 2008. Development of a three-dimensional, regional, coupled wave, current, and sediment transport model. Computers & Geosciences 34, 1284–1306.
Ward, L., Kemp, W., Boynton, W., 1984. The influence of waves and seagrass communities on suspended particulate matter in an estuarine embayment. Marine Geology 59, 85–103.
Wright, L.D., Boon, J., Xu, J., Kim, S.-C., 1992. The bottom boundary layer of the bay stem plains environment of lower Chesapeake Bay. Estuarine, Coastal and Shelf Science 35 (1), 17–36.
Young, I., Verhagen, L., 1996. The growth of fetch limited waves in water of finite depth. Part 1. Total energy and peak frequency. Coastal Engineering 29, 47–78.

Web References

Chesapeake Bay Program, 2011. Data Hub. http://www.chesapeakebay.net/dataandtools.aspx.
Halka, J., 2005. Surficial Sediment Distribution of Maryland's Chesapeake Bay. http://www.mgs.md.gov/coastal/vmap/baysed.html.
Maryland Department of Natural Resources, 2011. Chesapeake Bay Monitoring. http://www.dnr.state.md.us/bay/monitoring/index.html.
Scientific and Technical Advisory Committee, 2011. Evaluating the Design and Implementation of the Chesapeake Bay Shallow Water Monitoring Program. http://www.chesapeakebay.net/content/publications/cbp_13286.pdf.
United States Geological Survey, 2011. Chesapeake Bay: River Input Monitoring Program. http://va.water.usgs.gov/chesbay/RIMP/qwva_md.html.